

 Open access • Journal Article • DOI:10.1103/PHYSREVD.6.177

Phenomenology of Photon Processes, Vector Dominance, and Crucial Tests for Parton Models — [Source link](#)

Stanley J. Brodsky, Francis E. Close, J. F. Gunion

Institutions: Stanford University

Published on: 01 Jul 1972 - Physical Review D (American Physical Society)

Topics: Compton scattering and Parton

Related papers:

- [Gauge-Invariant Decomposition of Nucleon Spin](#)
- [Wave functions, evolution equations and evolution kernels from light ray operators of QCD](#)
- [Compton scattering and fixed poles in parton field-theoretic models.](#)
- [Factorization for hard exclusive electroproduction of mesons in QCD](#)
- [Nonforward parton distributions](#)

Share this paper:    

View more about this paper here: <https://typeset.io/papers/phenomenology-of-photon-processes-vector-dominance-and-2d8wiflh7>

PHENOMENOLOGY OF PHOTON PROCESSES, VECTOR DOMINANCE
AND CRUCIAL TESTS FOR PARTON MODELS*

Stanley J. Brodsky, Francis E. Close[†] and J. F. Gunion

Stanford Linear Accelerator Center
Stanford University, Stanford, California 94305

ABSTRACT

We discuss the phenomenological consequences of parton models for photon processes. In particular, the "breakdown" of vector meson dominance in Compton scattering is correlated with its failure in nuclear photoabsorption by showing that the parton model gives rise to a nonshadowed pointlike contribution which occurs only in two-photon processes. Included in this contribution is a piece which corresponds in the general Compton amplitude $T_{\mu\nu}$ to a term which is independent of energy and photon masses at fixed t . It is emphasized that failure to observe a contribution with such behavior would have profound consequences for conventional parton models. We predict that this contribution will have only a weak t dependence and will lead to a dominantly real spin conserving amplitude at large t values for Compton scattering. The q^2 behavior of this fixed pole is most easily detected in wide angle bremsstrahlung experiments, though the same mechanism will also give rise to an s -wave enhancement independent of the photon masses in $ee \rightarrow ee\pi\pi$.

(Submitted to Phys. Rev.)

* Work supported in part by the U. S. Atomic Energy Commission.

[†] NATO Fellow, 1970-1972.

I. INTRODUCTION

It has been known for some time that parton models provide a particularly physical and intuitive mechanism for the scaling in off shell forward Compton scattering. Application of this picture has, however, been restricted primarily to the large q^2 large ν region. In a recent paper we have discussed the extension of parton-field theoretic models for the Compton amplitude to all q^2 and ν and to the nonforward direction.¹ We found that a gauge-invariant treatment of the diagrams which yield scaling and point-like behavior for $\nu W_2(q^2, \nu)$ also results in an extra constant term (purely real) in the forward high energy Compton amplitude:

$$\frac{T_1^{\text{FP}}(q^2, \nu)}{T_1^{\text{Born}}} = \sum_a \int_0^1 dx \lambda_a^2 \frac{\tilde{f}_a(x)}{x} - \sum_{\alpha > 0} \frac{\gamma_\alpha}{\alpha} \quad (1)$$

where in the scaling region ($x = -q^2/2M\nu$)

$$\nu W_2 = \sum_a \lambda_a^2 x f_a(x) \xrightarrow{x \rightarrow 0} \sum_{\alpha > 0} x^{1-\alpha} \gamma_\alpha$$

and

$$\sum_a \lambda_a^2 \tilde{f}_a(x) = \sum_a \lambda_a^2 f_a(x) - \sum_{\alpha > 0} x^{-\alpha} \gamma_\alpha$$

(a = parton type; λ_a = parton charge). The particular diagrams associated with scaling behavior are a consequence of local electromagnetic interactions, occur specifically in scattering amplitudes involving two photons, and have no counterpart in photoproduction or purely hadronic amplitudes (we exclude the possibility that any of the hadrons are elementary). The absence of these diagrams for rho photoproduction and electroproduction coupled with their

presence in two photon processes will in fact play havoc with vector dominance relations. Some of the most interesting consequences of the extra pointlike diagrams are:

(1) The Compton amplitude will be predominantly real at high t . (Sections III and V.)

(2) S-channel helicity conservation will break down at high t in Compton scattering in such a way as to give a positive asymmetry parameter (Section IV).

(3) A slower falloff in the momentum transfer t in Compton scattering cross sections as compared to rho photoproduction is predicted (Section III).

(4) Amplitudes for two photon processes will fall off slowly as a function of the invariant masses of the photons. This will have dramatic implications for Bethe-Heitler wide angle pair production, bremsstrahlung (Section V) and colliding beam experiments (Section VI).

(5) An increasing lack of shadowing in the A dependence of the total (off shell) photoabsorption measurements on nuclei at high q^2 (Section VII).

(6) Despite the breakdown of vector meson dominance (VMD) in comparing $\gamma \rightarrow \gamma$ with $\gamma \rightarrow \rho$ processes, the relations between $\gamma \rightarrow \rho$ and $\rho \rightarrow \rho$ processes are not necessarily affected, and VMD results could still be reasonably good here (Section III).

Our purpose in this paper is to amplify upon the above mentioned implications of extended parton models for the phenomenology of general parton processes.

II. THE THEORETICAL MODEL

We first review for the reader the model we shall use, which in its basic form was first developed by Landshoff, Polkinghorne, and Short.² The implications of gauge invariance for the real part of the Compton amplitude and for

its extension to nonscaling regions is discussed below and in Ref. 1. Compton scattering is viewed as taking place via four basic covariant diagrams. The first (Fig. 1a) we shall refer to as the "six point" contribution, since the photons interact with the proton via a connected (in the sense that no freely propagating partons are present between the photons) off shell parton-parton-proton six point function.³ The next two (Figs. 1b and 1c) are the "four point" contributions, in which the parton propagates freely between the emission and absorption of the photons, and the last (Fig. 1d) we shall refer to as the "seagull" contribution (present as a separate diagram only for a spin 0 parton). Common to these last three diagrams is the four point parton-proton scattering amplitude. Each of the parton-proton four point and six point amplitudes is assumed to have normal hadronic behavior and to vanish as any of the parton four momenta squared becomes far off shell. (This last assumption is satisfied, for instance, in bound state models of the proton and in super-renormalizable field theories.) Figures 1b and 1c are the diagrams which give rise to a finite imaginary part in the scaling limit ($M\nu = p \cdot q \rightarrow \infty$, $q^2 \rightarrow \infty$, $\omega = 2M\nu/q^2$ fixed) due to the freely propagating parton lines. The six point contribution $T_{\mu\nu}^{(6)}$ vanishes in this limit. The seagull (or its spin 1/2 equivalent, an old fashioned perturbation theory Z graph evaluated in the infinite momentum frame) is totally independent of both ν and q^2 and thus survives in the scaling limit. It is, however, purely real and so, by the optical theorem, does not contribute to the total photoabsorption cross section. We thus have the following result for forward spin averaged Compton scattering in the scaling region at large ω ,⁴

$$T_1 = T_1^{(6)} + T_1^{(4)} \quad T_2 = T_2^{(6)} + T_2^{(4)} \quad (2)$$

with

$$T_1^{(6)} \approx 0 \quad \nu T_2^{(6)} \approx 0 \quad T_1^{(4)} = \sum_a \rho_\alpha \omega^\alpha \gamma'_\alpha + C$$

and

$$\nu T_2^{(4)} = \sum_a \rho_\alpha \omega^{\alpha-1} \gamma_\alpha - \frac{1}{\omega} C$$

where

$$T_{\mu\nu} = \left(-g_{\mu\nu} + \frac{q_\mu q_\nu}{q^2} \right) T_1 + \left(p_\mu - \frac{q_\mu p \cdot q}{q^2} \right) \left(p_\nu - \frac{q_\nu p \cdot q}{q^2} \right) \frac{T_2}{M^2}$$

and ρ_α = Regge signature factor. The so-called fixed pole term, C, of Eqs. (1) and (2) arises from the seagull (spin 0) or Z graph (spin 1/2) contribution and gives a contribution to $T_{\mu\nu}$ of the form ($T_1^{\text{Born}} = -2$)

$$(+2) g_{\mu\nu} \sum_a \lambda_a^2 \int_0^1 \frac{f_a(x)}{x} dx$$

The formal divergence at $x=0$ (originating from the fact that $f_a(x) \sim x^{-\alpha} \gamma_\alpha^a$ as $x \rightarrow 0$) is cancelled by a subtraction term which results when a subtracted dispersion representation is used for the leading Regge terms of the parton-proton $T^{(4)}$ amplitude. This results in the replacement of $f(x)$ by $\tilde{f}(x)$ and gives rise to the $-\frac{1}{\alpha} \gamma_\alpha$ term in Eq. (1). At $q^2=0$ the effects of the subtraction term disappear. The fixed pole may be calculated from either on or off shell data. (See Refs. 1 and 5.) The above expressions assume the simplest possible Regge behavior,

$$A(s, t=0) \rightarrow \sum_\alpha s^\alpha \beta_\alpha(\mu^2) \rho_\alpha \quad (3)$$

(s = four point function invariant energy, ρ_α = Regge signature, μ^2 = parton invariant (off shell) mass, $\beta_\alpha(\mu^2)$ = off shell dependent residue) for the

parton-proton amplitudes. The residues γ'_α and γ_α above may be computed in terms of $\beta_\alpha(\mu^2)$ (see Ref. 2). The Regge behavior of these amplitudes leads to Regge behavior in the Compton amplitude. We should emphasize that the $J=0$ fixed pole is generated by the local electromagnetic interactions, as we have assumed that the hadronic parton-proton amplitudes have only the normal $\alpha > 0$ Regge behavior. The fixed pole appears as a constant C in T_1 and $-C/\omega$ in νT_2 ; this combination being that which yields a total contribution (for perpendicular components) of the form $Cg_{\mu\nu}$, appropriate to a contact term in the full amplitude $T_{\mu\nu}$.⁶ The scaling Regge contributions to T_1 and νT_2 are related in this simple fashion only for spin 1/2 partons.

We turn now to the Regge region for the general Compton amplitude with q^2, q'^2 fixed, $\nu \rightarrow \infty$ (and, in general, $t \neq 0$ where $t = Q^2 = (q - q')^2$). It should be noted that both $T^{(4)}$ and $T^{(6)}$ diagrams contribute Regge terms. Consider first the $T^{(4)}$ four point contributions. We write the parton loop momentum k (see Figs. 1b and 1c) as $k = xp + yq + K$, where K is a spacelike vector perpendicular to both p and q . The basic hypothesis that the parton-proton amplitudes vanish if the virtual partons become far off shell implies that the dominant contributions to the Compton amplitude arise from regions of x and y where the parton invariant masses remain finite. In Figs. 1b and 1c these regions are $y=0$ and $x=0$.

The y near 0 contribution which survives in the scaling limit and yields the results of Eq. 2 gives a Regge contribution

$$T_{\mu\nu} = \bar{u}(p') M_{\mu\nu} u(p)$$

with

$$y \approx 0 M_{\mu\nu}^{(4)} = y \approx 0 R_{\mu\nu}^{(4)}(t, \nu, q^2, q'^2)$$

The q^2 dependent coefficients of the leading Regge terms are such that at large q^2 they result in the proper scaling behavior for the Regge terms. Inclusion of the subtraction term in the dispersion relation for the parton-proton amplitude is required.

In general, the fixed pole contributions from the seagull or Z-diagrams can be written in the form

$$M_{\mu\nu}^{\text{FP}} = 2g_{\mu\nu} \left[g_1(t) + g_2(t) \frac{2MK}{P \cdot K} \right] \quad (4)$$

where $K = \frac{q+q'}{2}$, $P = \frac{p+p'}{2}$, for perpendicular components μ, ν .⁶ The fixed pole always enters as a $g_{\mu\nu}$ term, and gives $(-2) [g_1(0) + g_2(0)]$ as the fixed pole's contribution to the forward spin-averaged on shell amplitude $T_1(q^2=0, \nu)$.

If we consider for simplicity the case of a spin zero external particle the fixed pole term is simply

$$T_{\mu\nu} = (+2)g_{\mu\nu} G(t) \quad (5)$$

where

$$G(t) = \sum_a \int_0^1 \frac{\lambda_a^2 \tilde{f}_a(x, t)}{x} - \sum_{\alpha > 0} \sum_a \frac{\gamma_\alpha^a(t) \lambda_a^2}{\alpha}$$

This is to be compared to the result for the form factor in such a case (Fig. 2)

$$\sum_a \int_0^1 \lambda_a f_a(x, t) = F(t) \quad (6)$$

The Pommeranchuk contribution to the parton-proton amplitude, which causes $f(x) \sim x^{-\alpha}$ for $x \rightarrow 0$ (with $\alpha = 1$) cancels when the sum over oppositely charged partons, a , is performed. As a result the integral in Eq. (6) does not diverge. As t becomes large the other Regge contributions rapidly disappear (having exponential residues in the parton-proton amplitude) leaving only contributions from background terms. The fixed pole, Eq. (5), is from the beginning only related to the background or nonleading portion of the x behavior. Because of this similarity, we expect that the fixed pole term will have a t dependence similar to that of the elastic form factor. (See Appendix I.) The expected falloff in t , perhaps similar to a dipole (t^{-2} at large t) is markedly slower than the exponential falloff expected for Regge terms.

In the case of spin we have

$$\langle p' | J_\mu | p \rangle = \bar{u}(p') \left[f_1(t) P_\mu + f_2(t) 2M \gamma_\mu \right] u(p) \quad (7)$$

as the defining equation for the form factors. Again, because of the similarity in structure between the elastic form factors f_1 , f_2 and g_1 , g_2 expect a slow falloff for the latter. (The fixed pole is, of course, controlled by $C = +$ exchanges as opposed to $C = -$ for the form factors.)

The four point x near 0 region yields a second Regge contribution to $M_{\mu\nu}$

$$x \approx 0 M_{\mu\nu}^{(4)} = x \approx 0 R_{\mu\nu}^{(4)}(q^2, q'^2, t, \nu) \quad (8)$$

which depends on q^2 and q'^2 in such a way that it vanishes as either q^2 or q'^2 becomes large.

The $T^{(6)}$ diagram also contributes a Regge term (arising from a single Regge limit of the parton-proton six point function depicted in Fig. 3) which we write as

$$M_{\mu\nu}^{(6)} = R_{\mu\nu}^{(6)}(q^2, q'^2, t, \nu) \quad (9)$$

This contribution also vanishes as either q^2 or q'^2 becomes large. In addition we note that no fixed pole arises from this latter type of diagram.

III. COMPTON SCATTERING AND VECTOR DOMINANCE

We turn now to the question of vector meson dominance. By definition the freely propagating parton diagrams (Figs. 1b and 1c) do not have poles in the photon channels. That is equivalent to saying that these diagrams cannot be vector meson dominated. On the other hand, the six point diagram is at least in part vector dominated. To decide to what extent we compare the processes $\gamma p \rightarrow \rho p$ and $\rho p \rightarrow \rho p$.

Only the six point diagrams contribute to these processes as interaction between the partons connected to the vector meson is necessary in order to bind them together. As a result we expect no fixed pole in either process.⁷ Experimentally a value for the coupling of $\gamma_\rho^2/4\pi = .65 \pm .01$ is required for vector dominance to work in going between the two processes.⁸ This is in agreement with the value $\gamma_\rho^2/4\pi \simeq 0.64$ measured directly by the Orsay experiment. We thus adopt as a working hypothesis vector dominance for the six point contribution.

In going from $\gamma p \rightarrow \rho p$ to $\gamma p \rightarrow \gamma p$ we can apply vector dominance only to the six point contribution. The presence of the additional four point Regge and fixed pole contributions is a general consequence of the parton model.⁹ In Fig. 4 we show a comparison of the VMD prediction for $\gamma p \rightarrow \gamma p$, using the $\gamma p \rightarrow V p$ data ($V = \rho, \omega, \phi$), $\gamma_\rho^2/4\pi = .65$, and the canonical 1/9:1:1/2 ratio for $\gamma_\rho^2:\gamma_\omega^2:\gamma_\phi^2$, with the actual data. It is clear that the agreement is poor. Not only is the forward normalization incorrect but also the shape at large t . The four point contributions are capable of explaining both these discrepancies. The fixed pole is small in magnitude⁵ and contributes only a few percent to the forward cross section, but both four point Regge contributions can be substantial.¹⁰ Indeed the comparison shows that these give about a 20% contribution for $q^2 = 0$. As t increases all Regge contributions can be expected to fall off rapidly in t (perhaps exponentially). The fixed pole will then eventually dominate due to its slower falloff. The change of shape in $\gamma p \rightarrow \gamma p$ (relative to $\gamma p \rightarrow \rho p$) is thus a reflection of the transition from Regge to fixed pole dominance occurring in that region of t . A complete discussion of the shape and energy dependence of $\gamma p \rightarrow \gamma p$ must, however, include the following important details.

(1) The four point Regge contributions, $R_{\mu\nu}^{(4)}$, will very probably be characterized by a gentler exponential t behavior than the six point Regge contributions. This is a result of the fact that the parton is a pointlike particle (as is required if it is to have no form factor, one of the key assumptions necessary to obtain scaling in a parton model). Unfortunately, different arguments lead to different conclusions as to just how much gentler this behavior should be. For instance if in proton-proton scattering the residue of a given Regge pole factorizes, (or if the residue results from a convolution of Gaussian constituent distributions)

then in GeV units

$$\gamma_{pp}(t) = \beta_{\text{proton}}(t) \beta_{\text{proton}}(t) \propto e^{-5|t|} \quad (10)$$

(experimentally $d\sigma_{pp}(t)/dt \propto e^{-10|t|}$ at small t and large energy). If the point-like nature of the parton results in replacing one proton residue with a t independent parton residue (or if the appropriate Gaussian radius of the parton is 0), then the appropriate t behavior for the parton-proton amplitude and hence for the four point Regge contributions will be

$$\gamma_4(t) = \beta_{\text{parton}} \beta_{\text{proton}}(t) \propto e^{-2.5|t|} \quad (11)$$

On the other hand it might be that a black disk picture is appropriate to proton-proton scattering in which case

$$\gamma_{pp}(t) = e^{-(R_p + R_p)^2 |t|} = e^{-4R_p^2 |t|} \quad (12)$$

i. e. , $R_p^2 = 1.25$ (R_p = proton radius) and

$$\gamma_4(t) \propto e^{-R_p^2 |t|} \simeq e^{-1.25|t|}$$

(Note that it is also not clear that, away from $t=0$, the four point Regge contributions need conserve helicity so that some helicity conservation violation might occur in the small t region.)

(2) Secondly the nature of the Pomeranchuk trajectory, P , becomes crucial. If it is true that it, as well as the $f-A_2$ trajectory, has a positive slope then at large t its energy dependence will be governed by an effective $\alpha < 0$. (Presumably, however, there are P^n and $R \cdot P^n$ cuts which will take longer to fall below zero.¹¹) The fixed pole will then give the leading energy dependence and higher

energy will make it easier to see. If on the other hand, the Pomeranchuk trajectory is flat, increasing the energy at large t will only help for the n-p difference, from which it will be possible to measure the difference between the neutron and proton fixed pole residues.

(3) Finally, we must consider the possibility that an additional process exists which could influence the $\gamma-\gamma:\gamma-\rho$, $\frac{d\sigma}{dt}$ comparison; namely that strongly interacting massive vector gluons could be exchanged between the parton and the proton in the parton-proton amplitude. Proton-proton scattering at large t can be reasonably well described¹² by such a vector gluon exchange between the protons (leading to $A \sim is * G_M^2(t)$ (Ref. 13)). Here only one proton is present, giving $A \sim is * G_M(t)$. Only even charge conjugation vector exchanges (i.e., $J^P = 1^+$) survive in the even charge conjugation Compton amplitude, so that even if such a term is present in the proton-proton scattering amplitude it need not be present in the Compton amplitude. However, if a vector gluon is present, it will have as weak a t dependence as the fixed pole whose constant behavior in s will be overshadowed by the gluon's linear s dependence. The effect of such a term would thus be quite dramatic and it should be evident at present energies. The fit referred to below, however, does not seem to require such a contribution in addition to the normal Regge trajectories.

In Fig. 4 we have shown a sample fit to $\gamma p \rightarrow \gamma p$ which includes, in a simple fashion,¹⁴ the above considerations. Also shown is the vector dominance prediction.

Thus large t is certainly required to see the fixed pole directly. Note that if trajectories have positive slope, increasing the energy will help provided t is such that all Regge trajectories and cut intercepts lie below zero. Given the uncertainty in the Pomeranchuk slope it is difficult to estimate a t value for which

this might happen. One should first try looking for the fixed pole at the presently available energies by going to large t ($|t| > 1.5 \text{ GeV}^2$ would for instance be sufficient for the fit of Fig. 4). The direct observation at large t of this constant term in Compton scattering would be a striking confirmation of the parton picture.

IV. ASYMMETRY PARAMETER

In the region where the fixed pole dominates the Regge terms, it is possible to make a definite prediction which will be testable in the near future (when experiments at $|t| > 1.5 \text{ GeV}^2$ are done) and will provide a check of this picture.

It is clear from Eq. (4) that the fixed pole results in a contribution to the on shell Compton amplitude of the form

$$-2 \vec{\epsilon}'^* \cdot \vec{\epsilon} \bar{u}(p') \left[g_1(t) + g_2(t) \frac{2M\mathcal{K}}{P \cdot K} \right] u(p) \quad (13)$$

which as we have said will dominate the amplitude at large t . (ϵ and ϵ' are the helicity 1 (or -1) photon polarization vectors.) Such a term can be detected (independently of the nucleon spin unknowns) by measuring the asymmetry parameter

$$A = \frac{\sigma_{\perp} - \sigma_{\parallel}}{\sigma_{\perp} + \sigma_{\parallel}} = \frac{2 \sum_{\lambda\lambda'\lambda'_\gamma} \text{Re} (f_{1\lambda\lambda'\lambda'_\gamma} f_{-1\lambda\lambda'\lambda'_\gamma}^*)}{\sum_{\lambda\lambda'\lambda'_\gamma} \left[|f_{1\lambda\lambda'\lambda'_\gamma}|^2 + |f_{-1\lambda\lambda'\lambda'_\gamma}|^2 \right]} \quad (14)$$

(λ, λ' ; λ'_γ are the helicities of the initial and final nucleons and of the final state photon respectively) between the cross sections for photons polarized perpendicular and parallel to the scattering plane. The resulting A will be of the form

$$A = \frac{\sin^2 \theta}{1 + \cos^2 \theta} \quad (15)$$

(θ = laboratory scattering angle). Polarization information for the initial photon only is required.

V. DIRECT MEASUREMENTS OF THE REAL PART OF THE COMPTON AMPLITUDE

Direct measurements of the Compton amplitude's real and imaginary parts are possible by using the processes

$$e^\pm p \rightarrow e^\pm p \gamma \qquad q^2 = (p_e - p'_e)^2$$

or

$$\gamma p \rightarrow e^+ e^- p \qquad q^2 = (p_e + p'_e)^2$$

involving spacelike and timelike photons respectively. Such measurements are crucial in testing the predictions of the parton model, as they check the resulting $t = (P - P')^2$ and q^2 dependence of the real fixed pole contribution in the T_1 amplitude. The latter process was examined in Ref. 15; here, we examine the former. This ability to test the contact nature of the fixed pole directly by studying the properties of the real part at large t is particularly important in view of the uncertainties encountered when attempting to extract the real part from a measurement of the differential cross section for Compton scattering.

We consider the processes depicted in Figs. 5a, b, and c, which contribute to wide angle bremsstrahlung emission of one photon in the scattering of an electron or positron from a nucleon. Although we have worked out the full expression for the elastic bremsstrahlung cross section based on Eq. (13) for the fixed pole, we shall just give here the results for a small angle kinematic region, where the effect of the Compton amplitude is simple to analyze. Let θ_k , θ' , k_0 , E' be the laboratory angles and energies of the final photon and lepton (see Fig. 5). The important parameters of the problem are t , the

momentum transfer to the nucleon, and q^2 , the mass of the initial photon in the Compton scattering portion of Fig. 5c. One should note that these can be adjusted independently as they depend on different laboratory angles, θ_k and θ' respectively. Isolation of the fixed pole contribution to Compton scattering will require large t , i. e., large $E-E'$ and a reasonable value of θ_k . Large $E-E'$ is also required in order to be in the Regge region of the Compton amplitude, i. e., at large ν , where the fixed pole is relevant. On the other hand, the q^2 dependence of the Compton amplitude's real part may be studied by varying θ' . For orientation we first consider the case of spinless particles. The standard Bethe-Heitler contribution (from Figs. 5a, b plus the spin zero seagull contribution) is

$$M_{\text{BH}} = \frac{2M_p F(t)}{t} \left[\frac{(2p'_e + k) \cdot \epsilon(E + E' + k_0)}{2p'_e \cdot k} + \frac{(2p_e - k) \cdot \epsilon(E + E' - k_0)}{-2k \cdot p_e} - 2\epsilon_0 \right] \quad (17)$$

where $F(t)$ is the nucleon form factor. Only photons linearly polarized in the electron scattering plane contribute. Keeping only leading terms in the angles, neglecting recoil and choosing $\theta_k^2 \gg \theta'^2$ (which will emphasize the Compton interference contribution) we obtain

$$M_{\text{BH}} = - \frac{8M_p F(t)}{k_0^2 \theta_k^3}$$

using $\epsilon^\mu = (0, 1 - \theta_k^2/2, 0, -\theta_k)$ and $k_0 \cong E - E'$. Next consider the contribution of Fig. 5c, which becomes the fixed pole g_{ij} seagull contribution at large t . The

corresponding contribution to the bremsstrahlung amplitude is

$$M_s = -2 \left(\frac{T_1^{\text{FP}}}{T_1^{\text{Born}}} \right) G(t) \left(\frac{(p_e + p'_e) \cdot \epsilon}{q^2} \right) \quad (19)$$

$$\cong 2 \left(\frac{T_1^{\text{FP}}}{T_1^{\text{Born}}} \right) G(t) \left(\frac{(E + E') \theta_k}{EE' \theta^2} \right)$$

where $T_1^{\text{FP}}/T_1^{\text{Born}}$ is given by Eq. (1) and $G(t)$ is the spinless fixed pole form factor. [We can also compute the contribution of Fig. 5c for the case in which t is small and q^2 is small. The result is obtained from Eq. (19) by replacing $G(t)T_1^{\text{FP}}$ by T_1 . (At $q^2=0$ and $t=0$ only one invariant amplitude, T_1 , enters.) In this case the real part of T_1 will obviously have $f\text{-}A_2$ Regge contributions in addition to the fixed pole.] Hopefully, the complications of the Pomeron and/or vector gluon would be present mainly in the imaginary part of T_1 , which as we shall see will not enter. We refer to the contribution of Figs. 5a and 5b as B , and that of Fig. 5c as S ; we note that S changes sign when $e^+ \rightarrow e^-$ (we have presented the results for the e^+ case above), while B does not. Thus if we measure

$$R = \frac{\sigma_+ - \sigma_-}{\sigma_+ + \sigma_-} = \frac{|B+S|^2 - |B-S|^2}{|B+S|^2 + |B-S|^2} = \frac{2B \text{Re } S}{|S|^2 + |B|^2} \quad (20)$$

(note: B is purely real) it will be possible to obtain information concerning $\text{Re } S$. In fact, if one inserts reasonable values for the energy and angles (keeping the angles < 25 degrees, say), then $|B|^2 \gg |S|^2$ and we have

$$R = - \frac{T_1^{\text{FP}}}{T_1^{\text{Born}}} \frac{G(t)}{F(t)} \frac{1}{2M} \frac{(E+E')(E-E')^2}{EE'} \frac{\theta_k^4}{\theta'^2} \quad (21)$$

The result for spin 1/2 leptons on spin 1/2 nucleons is very similar in this kinematic region since only the convection parts of the nucleon current and fixed pole are operating. We get

$$R = \frac{2 \operatorname{Re} S}{B} = - \left(\frac{g_1(t) + g_2(t)}{G_E(t)} \right) \frac{\theta_k^4 (E-E')^2}{\theta'^2 (E+E')} \frac{2}{M}$$

with

$$g_1(0) + g_2(0) = \frac{T_1^{\text{FP}}}{T_1^{\text{Born}}}$$

and $G_E(t)$ is the electric form factor of the proton.

It is desirable to examine this result in two cases.

(1) At large t , where the fixed pole is expected to dominate, one can determine the following from a measurement of R : (a) whether or not the Compton amplitude is, indeed, independent of energy; (b) just what the magnitude of the fixed pole is; and (c) whether this constant term is in fact q^2 independent (i. e. , whether R depends on θ' only via the $1/q^2$ of the photon propagator). This last is the most important test of the theoretical concepts embodied in the parton model.

(2) At small t and $q^2 = 0$ (i. e. , θ_k small and $\theta' \rightarrow 0$), one can also hope to measure $\operatorname{Re} T_1(t=0)$ in the Regge region to sufficient accuracy that separation of the $f-A_2$ and fixed pole contributions might be possible. Observation of terms in the real part of T_1 which do not conform to this interpretation would be of great theoretical consequence.

The importance of direct measurements of the real part of the Compton amplitude in the manner suggested above cannot be overly stressed. It provides one of the only direct tests of the theory herein discussed.

VI. FURTHER CONSEQUENCES OF THE SEAGULL CONTRIBUTION

In the previous section we have illustrated the importance of the seagull-type contribution to wide angle bremsstrahlung and how this process serves as a critical test of the fundamental ideas of the parton model. This seagull contribution is expected to be important in all two photon processes which involve hadrons. For example, new tests of the nature of parton contributions to two photon amplitudes

$$\gamma + \gamma \rightarrow \text{hadrons}$$

(for spacelike photons) are possible from measurements of the process $ee \rightarrow ee + \text{hadrons}$. In particular, the seagull—fixed pole—contribution yields an s-wave contribution to $\gamma + \gamma \rightarrow \pi^+ \pi^-$ pair production which is independent of photon mass for any fixed $s = m_{\pi^+ \pi^-}^2$. In general, we emphasize the importance of including in all $\gamma\gamma$ processes the parton ($T^{(4)}$ + seagull) contributions which are of point-like nature.

VII. SHADOWING IN PHOTONUCLEAR INTERACTIONS

The phenomenological picture that we have developed has interesting consequences for the total photoabsorption cross sections on nuclei. Direct application of the simplest rho dominance model to the forward elastic amplitude for photons on nuclei, together with the optical theorem, would predict (at large energy)¹⁶

$$\sigma_{\gamma A} \propto \sigma_{\rho A}$$

This latter cross section will behave like A^n with $n < 1$ because of the shadowing effect arising from the relatively short mean free path of rho's in nuclear matter. Indeed if $\sigma(\rho N) = \infty$ then the ρ would see only the surface of the nucleus and

we would have

$$\sigma_{\rho A} \sim A^n \sigma_{\rho N}$$

with $n=2/3$. For the observed total cross section magnitudes one finds $2/3 < n < 1$, the precise value depending upon the explicit magnitude of $\sigma(\rho N)$ and upon the scattering energy. The "direct" measurement from ρ -photoproduction on deuterium of Anderson et al.¹⁷ yields $\sigma(\rho N) \sim 26$ mb and $\gamma_\rho^2/4\pi \sim .65$ at large ν , in excellent agreement with the quark model result

$$\sigma_{\rho N} = \frac{1}{2} [\sigma(\pi^+ N) + \sigma(\pi^- N)] .$$

Using these values and a ratio of real to imaginary contribution of -0.2 in the $pp \rightarrow \rho p$ 16 GeV scattering amplitude leads one to expect $\sigma(\rho A) \sim A^{.89}$. Vector dominance would then predict $\sigma(\gamma A)/\sigma(\gamma N) \sim A^{.89}$.¹⁸

The data¹⁹ for the A dependence of photoabsorption cross sections of on shell photons by nuclei is shown in Fig. 6. The data show a more linear dependence of $A_{\text{eff}} (= \sigma(\gamma A)/\sigma(\gamma N))$ upon A than that given by the vector dominance result. Were the photon pointlike, in the sense that it had a long mean free path in the nucleus, one would predict $\sigma(\gamma A) \sim A\sigma(\gamma N)$. The data thus indicate the presence of such a "piece" in the photon. This is precisely what we expect from our theoretical model. (The solid curve in Fig. 6 is the result of the calculation which follows.)

In Section III we noted that while VMD worked beautifully in comparing $\gamma p \rightarrow \rho p$ with $\rho p \rightarrow \rho p$, it failed to agree with the $\gamma p \rightarrow \gamma p$ data. In particular the predicted magnitude of the forward differential cross section for on shell Compton scattering (including omega and phi contributions) is $\sim 0.41 \mu\text{b}/\text{GeV}^2$ at 16.6 GeV, whereas the known value of $\sigma_T(\gamma p)$ at this energy, or extrapolation

of the $\gamma p \rightarrow \gamma p$ data to $t=0$, yields a forward cross section of about $0.68 \mu\text{b}/\text{GeV}^2$. This difference we accounted for by noting the existence of the $T^{(4)}$ diagrams which were not vector dominated. If we assume the same ratio of real to imaginary part in the $T^{(4)}$ as in the $T^{(6)}$ contribution (apart from the fixed pole which is negligible in the forward direction anyway) we obtain

$$\frac{\sigma_T^{T^{(4)} + T^{(6)}}(\gamma N)}{\sigma_T^{T^{(6)}}(\gamma N)} = \frac{\sigma_T^{\text{Data}}(\gamma N)}{\sigma_T^{\text{VMD}}(\gamma N)} = \sqrt{\frac{\frac{d\sigma^{\text{Data}}}{dt}(\gamma N \rightarrow \gamma N)}{\frac{d\sigma^{\text{VMD}}}{dt}(\gamma N \rightarrow \gamma N)}} \sim \frac{1}{.78} \quad (22)$$

(This ratio is empirically constant over the range of energies 5 GeV - 17 GeV which is to say that the energy behavior of the $T^{(4)}$ and $T^{(6)}$ Regge contributions is the same, as we would expect from our theory.) $T^{(4)}$ diagrams correspond to cases in which the photon is absorbed and reemitted by the same nucleon and thus correspond to a pointlike piece of the photon, for which the A dependence is linear as discussed. In Appendix II we argue that this contribution to the one step process is negligibly shadowed by its corresponding two step process (Fig. 7b) because of the relatively small size of the parton-proton cross section and because of the off shell parton effects in the intermediate state (for the diffractive region). Using the single nucleon ratio

$$\sigma(\gamma p) \sim .22 \sigma_{T^{(4)}}(\gamma p) + .78 \sigma_{T^{(6)}}(\gamma p) = .22 \sigma(\text{pointlike}) + .78 \sigma(\text{VMD}) \quad (23)$$

and using the A dependence expected for the vector dominated piece given above we find

$$\frac{\sigma(\gamma A)}{A\sigma(\gamma N)} \sim .22 + .78 A^{(.89-1)} \quad (24)$$

(We have ignored in all this the difference between p and n cross sections²⁰ which is about 5% at this energy and will have only a small effect.) This curve is plotted in Fig. 6 and agrees remarkably well with the data. For lead A=207, the correction results in about a 20% increase in the ratio above that expected from pure VMD. This effect can also be parameterized as an increase of the one step process relative to the two step above the value predicted by VMD. suri and Yennie²¹ have noticed that numerically that this is what is required to make theory agree with experiment. Here we have shown that a natural physical picture makes it clear that such an adjustment should indeed be necessary and in addition relates the approximate magnitude of the effect to single nucleon data. The success of this procedure is clear evidence for the existence of pointlike interactions of the photon such as incorporated in this theory.

It also seems that shadowing disappears when absorption of off shell ($q^2 > .3 \text{ GeV}^2$) photons is examined. Recent data²² on Cu and Be targets show no sign of shadowing. This is precisely what should happen once the six point vector dominated contributions become small relative to the scaling contributions of the four point function. These latter diagrams will not exhibit absorption as the photon is reemitted before absorption can occur. In addition, the early (i. e. , small q^2) on set of scaling, if taken as evidence for the early vanishing of the nonscaling six point contributions, indicates that by $q^2 = .5$ the predominant contributions are the unshadowed four point contributions which are not vector meson dominated.

This differs somewhat from the picture proposed by Harari.²³ The analysis of Ref. 5 suggested that $\nu = 2 \text{ GeV}$ at $q^2 = 0$ is to be compared with ν near 50 GeV when $q^2 = 1$, and Harari proposes that shadowing observed in the latter region might be similar to that observed at $q^2 = 0$, $\nu = 2$. From our point of view this

would require that there be Regge pieces of the $T^{(6)}$ amplitudes which scale at values of $q^2=1$ provided the energy ν is great enough. (This is similar to the point of view of suri and Yennie.) We cannot rule out this possibility but the present model suggests an alternative in which the off shell physics and cross sections appropriate to the relevant two step processes are such as to greatly reduce the shadowing even when the energy ν is large compared to q^2 .

Thus we have presented a physically intuitive basis for an understanding of the transition from $q^2=0$ to large q^2 . At $q^2=0$ the VMD dominated diagrams Figs. 1a and 3 account for about 80% of the observed contribution in the near forward direction, whereas at either large q^2 or at large t , VMD will fail due to the dominance of the other diagrams.

VIII. CONCLUSIONS

We have presented a picture for Compton scattering (and, of course, nuclear photoabsorption) which is based upon one possible theoretical explanation of exact scaling. The characteristic feature of the model used is that it provides a smooth interpolation between the Regge and the scaling regions, such that the freely propagating parton amplitude (which dominates in the scaling region) does not become totally irrelevant in the nonscaling region even though in this latter region other contributions are equally or more important in most cases. It is not impossible that the scaling observed at SLAC represents the effects of a theory which is totally irrelevant at smaller q^2 . In such a case, however, a smooth interpolation between the Regge region and the scaling region would not exist in the sense that the physics appropriate at high q^2 would have no effect at low q^2 . We have shown that there is some experimental support for a theory in which the physics is not discontinuous, and that in the very near future it

will be possible to perform detailed experimental tests of the picture provided by such a theory. The most important such test is provided by measurements of electron-positron wide angle bremsstrahlung $e^\pm p \rightarrow e^\pm p \gamma$. Measurements at small t and small $q^2 = (p_e - p'_e)^2$ directly determine the real part of the Compton amplitude and thus will help in separating the fixed pole from the Regge terms. At high t only the former "seagull" contribution, characteristic of the parton model, survives in the Compton amplitude's real part. Verification of q^2 independence (at fixed t) of this $J=0$ fixed pole contribution would be dramatic evidence supporting the local structure of electromagnetic interactions implicit in the parton model. However, if q^2 dependence of the $J=0$ fixed pole is observed, then the field-theoretic parton model would be destroyed.

ADDENDUM

After this paper was completed, we received a paper by D. O. Caldwell et al. (University of California, Santa Barbara, unpublished) in which is noted the need for a short range electromagnetic interaction in nuclear photoabsorption.

ACKNOWLEDGMENTS

We wish to thank our colleagues at SLAC for helpful discussions, in particular J. D. Bjorken, F. J. Gilman and A. suri. One of us (FEC) wishes to thank the Science Research Council of London for administering a NATO fellowship.

REFERENCES AND FOOTNOTES

1. S. J. Brodsky, F. E. Close, J. F. Gunion, Report No. SLAC-PUB-973 and in preparation.
2. P. Landshoff, J. C. Polkinghorne and R. Short, Nucl. Phys., B28, 225 (1971).
3. In the case of composite field theory models of the proton it is important to realize that the six point diagram includes certain diagrams in which one photon interacts with the bare proton, while the other interacts via the full vertex function. These are necessary for the gauge invariance of T_2 (for instance, they cause the fixed pole residue in T_2 to be linear in q^2).
4. For the expressions in other ω regions see Ref. 2.
5. F. E. Close and J. F. Gunion, Phys. Rev., D4, 742 and D4, 1576 (1971); J. M. Cornwall, D. Corrigan and R. Norton, Phys. Rev. Letters, 24, 1141 (1970).
6. In general, if one looks at components μ and ν for which neither $P_{\mu,\nu}$ nor $K_{\mu,\nu}$ are of order $\nu = \frac{P \cdot K}{M}$ ($P = \frac{p+p'}{2}$, $K = \frac{q+q'}{2}$; p, p', q, q' are the initial, final proton-photon momenta respectively) then only terms proportional to $g_{\mu\nu}$ survive as energy independent contributions in the amplitude. When considering processes involving longitudinally polarized photons one must take into account the fact that the fixed pole actually occurs in an invariant amplitude which multiplies a fully gauge-invariant tensor. In Appendix I this point is clarified and the gauge-invariant form of the contact term discussed.

7. This argument can be turned around as well. Theoretically one does not expect fixed poles in $\rho p \rightarrow \rho p$ as it is a purely strong process. If vector dominance is to work in going from $\rho p \rightarrow \rho p$ to $\gamma p \rightarrow \rho p$ there can be no fixed poles in this latter process either. Cheng and Tung (Phys. Rev. Letters, 24, 851 (1970)) show that in this case a fixed pole with polynomial residue will occur in $\gamma p \rightarrow \gamma p$. The present theory avoids these arguments and shows that the polynomial residue is the simplest possible one, i.e., one which "scales".
8. R. Anderson et al., Phys. Rev., D1, 27 (1970); G. Wolf, Rapporteur talk at the 5th International Conference on Electron and Photon Interactions at High Energy, Cornell, 1971.
9. This is similar to the observations by Suri and Yennie who assume the existence of a "short range" contribution to Compton scattering in addition to the vector-dominated pieces. Their short range piece does not include any leading Regge behavior. Regge behavior, however, is natural for the non-vector-dominated contributions in our model. Zyan F. Ezawa, Phys. Rev. Letters, 27, 1092 (1971) has also noted the presence of non-vector-dominated contributions in Compton scattering.
10. Duality, applied to the parton-proton amplitudes, tells us that the sign of each Regge term's imaginary part is positive, for both four and six point contributions. (Hence they will add in phase.) The actual size of the four and six point Regge terms is, however, model dependent. For instance, the y near $0 T^{(4)}$ Regge contribution for q^2 not large cannot be estimated from scaling region data, the extrapolation depending on an unknown spectral function in the form

$$\int \frac{\rho(m^2) dm^2}{(q^2 + m^2)^\alpha} \alpha^{(2\nu)^\alpha} .$$

11. Effective trajectories for the totality of such contributions have been given by H. Yabuki, Phys. Rev., 177, 2209 (1969). They are of the form $A - b \sqrt{-t}$, if the original trajectories are linear in t .
12. H. Abarbanel, S. D. Drell and F. J. Gilman, Phys. Rev., 177, 2458 (1969).
13. In the absence of important unitarity corrections, a gluon term, linear in s , can only contribute to the imaginary part of the amplitude (i. e., it must have positive signature) if the Pomeranchuk theorem, equality of particle and antiparticle cross sections at high energy, is not to be violated.
14. Unfortunately the t behavior and real parts of the various Regge terms are subject to great ambiguity so that no definitive statement can be made in this t range. The naive fit was made by assuming the additional Regge terms merely renormalized the total Regge contribution (continuing to preserve s -channel helicity conservation) so as to agree in the forward direction. The t dependence of these terms was assumed to be approximately $\exp(-2t)$ in the amplitude. A fixed pole with electromagnetic dipole form factor t dependence was then added in. An equally good parameterization results when the $T^{(4)}$ Regge terms are replaced by a gluon type term is $*A(t)$ where $A(t)$ has a t dependence like the electromagnetic form factor $G_M(t)$. This last point indicates the impossibility at present t values of deciding whether or not such a gluon term is, in fact, important.
15. S. J. Brodsky, A. C. Hearn, and R. G. Parsons, Phys. Rev., 187, 1899 (1969).

16. More rigorously vector dominance predicts that at high energies, $\nu \gg (m_\rho^2 + Q^2) \cdot d$, the two step amplitude in Compton nuclear scattering coherently shadows the one step amplitude for scattering on the interior nucleons.
17. R. Anderson, et al., Report No. SLAC-PUB-916.
18. S. J. Brodsky and J. Pumplin, Phys. Rev., 182, 1994 (1969); K. Gottfried and D. R. Yennie, Phys. Rev., 182, 1595 (1969) and references therein.
19. D. O. Caldwell, et al., Phys. Rev. Letters, 23, 1256 (1969); see also K. Gottfried, Rapporteur talk at the Cornell conference (1971) (see Ref. 8).
20. This is obtained from the deuterium data.
21. A. suri and D. Yennie, contribution to the Cornell conference (Ref. 8).
22. See e.g., H. Kendall, Rapporteur's talk at the 1971 Cornell Conference (Ref. 8).
23. H. Harari, Rapporteur talk at the 1971 Cornell Conference (Ref. 8), and private communication.
24. S. D. Drell, D. Levy and T. M. Yan, Phys. Rev., 187, 2159 (1969); ibid., D1, 1035 (1970).
25. R. L. Anderson, et al., Phys. Rev. Letters, 25, 1218 (1970); A. M. Boyarski, et al., Phys. Rev. Letters, 26, 1600 (1971).

FIGURE CAPTIONS

1. The covariant diagrams contributing to the Compton amplitude. In the text these are referred to as (a) six point or $T^{(6)}$, (b) and (c) four point or $T^{(4)}$, (d) seagull. Figure (d) is separable from (b) and (c) only for spin zero partons (see text and Ref. 1).
2. The elastic form factor.
3. The single Regge limit of the $T^{(6)}$ diagram appropriate in the Regge region of Compton scattering. Also shown schematically is the vector dominance hypothesis for this diagram, which relates (a) $\gamma\gamma$ to (b) γV , and to (c) VV . Vector dominance applies only to the $T^{(6)}$ diagrams.
4. Compton scattering at 16.6 GeV/c (data from Ref. 25). The lower of the curves labelled VMD is the result of taking the vector meson photo-production data of Ref. 8 and using $\gamma_\rho^2/4\pi = 0.65$ (see text). (This of course is the Orsay value and is also that which works well in predicting γV from VV data; see Fig. 4b where we show a sample comparison between this latter VMD prediction and the γV data.) Renormalizing this curve so as to agree at small t yields the upper VMD curve (corresponding to $\gamma_\rho^2/4\pi = 0.35$). The curve labelled BCG is that described in footnote 14.
5. The Feynman diagrams contributing to the process $ep \rightarrow ep\gamma$ to lowest order in e . Diagrams (a) and (b) are the Bethe-Heitler processes, and (c) is the Compton contribution. Note that when $e^+ \rightarrow e^-$, diagram (c) changes sign whereas (a) and (b) are unchanged.
6. Shadowing in 14.4-18.3 GeV on shell nuclear photoabsorption.
 $A_{\text{eff}} = \sigma(\gamma A)/\sigma(\gamma N)$ for a nucleus containing A nucleons.

"No shadowing" would predict $A_{\text{eff}} \sim A$ (the upper curve) while the vector dominance model with $\sigma(\rho N) = 26 \text{ mb}$ and a ratio of 20% for the real part of the $\gamma \rightarrow \rho$ amplitude to its imaginary part yields the lower curve ($\gamma_{\rho}^2/4\pi = 0.65$). The curve labelled BCG is given by $0.22 A + 0.78 A^{.89}$ (see text), corresponding to the 22% pointlike portion expected on the basis of the model of the text.

7. Nuclear shadowing of the four point contribution to Compton scattering.
 - (a) The deuteron becomes two nucleons and the Compton scattering takes place on a parton of one nucleon, the parton being reabsorbed by the same nucleon. The nucleons then recombine to form the deuteron.
 - (b) The process that might shadow the pointlike one of (a). In this case the parton which is involved in the Compton scattering is reabsorbed by a different nucleon than that from which it was emitted. In addition a second parton travels between the two nucleons.

APPENDIX I

We have stated that the characteristic feature of the fixed pole is that if one examines, the amplitude $T_{\mu\nu}$ with μ and ν chosen such that none of the external momenta have components of order $P \cdot K = \nu$ in either the μ or ν direction, then the constant $\alpha = 0$ fixed pole (F. P.) appears as a term proportional to $g_{\mu\nu}$. This can be derived by examining the properties of the graphs which gave rise to this high energy constant real part in a parton model. The seagull graphs, for spin 0, and the old fashioned perturbation theory Z graphs (evaluated in the infinite momentum frame), for spin 1/2 partons, each have this property. When examining the amplitude $T_{\mu\nu}$ for other components $\mu\nu$ (e.g., when computing quantities involving longitudinally polarized photons) it becomes necessary to realize that the fixed pole is gauge invariant in the sense that it occurs in one or more invariant amplitudes multiplying gauge invariant tensors.

When the external particle has spin 0 (or when we consider a spin averaged amplitude) there are, in general, 5 independent gauge invariant tensors, and correspondingly 5 invariant amplitudes, for nonforward scattering of unequal mass photons. The fixed pole occurs in only one of these. The associated gauge invariant tensor (see Bardeen and Tung, Phys. Rev., 173, 1423 (1968)) we write as

$$\mathcal{L} = g^{\mu\nu} (P \cdot K)^2 - K \cdot P (K^\mu P^\nu + P^\mu K^\nu) + k \cdot k' P^\mu P^\nu \quad (\text{I. 1})$$

where $P = \frac{p+p'}{2}$ is the average of the initial and final nucleon momenta, and $K = \frac{k+k'}{2}$ where $\epsilon^\nu(k)$ and $\epsilon^\mu(k')$ are the initial and final photons. The amplitude Reggeises as $\nu^{\alpha-2}$, ($\nu = P \cdot K$).

The $\alpha=0$ fixed pole cannot occur in any of the other four invariant amplitudes as this would lead to terms in $T_{\mu\nu}$ which are not proportional to $g_{\mu\nu}$ (for μ and ν chosen as stated above). \mathcal{L} is the only tensor in which the terms which restore gauge invariance to $g^{\mu\nu}$ are explicitly $1/\nu$ relative to the $g^{\mu\nu}$ term.

For spin 1/2 external nucleons there are no less than 18 gauge invariant tensors in the nonforward direction. The fixed pole can occur multiplying only two of these, namely.

$$\begin{aligned} \mathcal{L}_1 = & K^2 P^\mu P^\nu - K \cdot P (K^\mu P^\nu + P^\mu K^\nu) \\ & - \frac{1}{2} \left[(P^2 K^2 - (P \cdot K)^2) \right] g_{\mu\nu} + P^2 K^\mu K^\nu \end{aligned} \quad (I.2)$$

and

$$\begin{aligned} \mathcal{L}_2 = & K^2 (\gamma^\mu P^\nu + P^\mu \gamma^\nu) - K \cdot P (K^\mu \gamma^\nu + \gamma^\mu K^\nu) \\ & - \gamma \cdot K (K^\mu P^\nu + P^\mu K^\nu) + K \cdot P \gamma \cdot K g^{\mu\nu} - m K^2 g^{\mu\nu} + P^2 K^\mu K^\nu \end{aligned}$$

(the associated invariant amplitudes Reggeize as $\nu^{\alpha-2}$). Again, the other invariant tensors do not have the property that an $\alpha=0$ fixed pole occurring in the corresponding amplitude would be proportional only to $g_{\mu\nu}$ when μ and ν are chosen as stated earlier. When examining such μ and ν components we have

$$T_{\mu\nu}^{\text{FP}} = \bar{u}(p') M_{\mu\nu}^{\text{FP}} u(p) \quad \text{with} \quad M_{\mu\nu}^{\text{FP}} = \frac{4g_1(t)}{\nu^2} \mathcal{L}_1 + \frac{4Mg_2(t)}{\nu^2} \mathcal{L}_2 \quad (I.3)$$

which to leading order in ν reduces to Eq. 4 of the text.

Finally we wish to note that in an infinite momentum frame the local parton operators for the fixed pole and form factor are merely related by (for either spin 1/2 or spin 0 parton)

$$O_{\text{Fixed Pole}} = \frac{g_{\mu\nu}}{x_a} O_{\text{Form Factor}} \quad (\text{I.4})$$

(x_a being the fraction of longitudinal momentum of parton a). Thus we expect that parton by parton the contribution to the form factors of a spin 1/2 nucleon will be related by

$$\frac{f_1^a}{f_2^a} = \frac{g_1^a}{g_2^a} = \lambda \quad (\text{I.5})$$

Since

$$f_i = \sum \lambda_a f_i^a$$

$$g_i = \sum \lambda_a^2 g_i^a$$

this relation will be preserved for the full form factors of a spin 1/2 nucleon.

We note further that the Drell-Yan relation, which correlates the asymptotic behavior of the elastic form factors f_i with the behavior of the structure function $F_2(x) = xf(x)$ at x near 1, implies that the g_i^a form factors have the same asymptotic t dependence as the f_i^a because of Eq. (I.4).

APPENDIX II

In this appendix we explain why the single step $T^{(4)}$ process (illustrated for a deuteron in Fig. 7a) is only negligibly shadowed by its corresponding two step process (Fig. 7b). There are two effects which tend to reduce the importance of the two step process, either one of which would be sufficient on its own.

First of all, the shadowing will be substantial only if the parton-nucleon total cross section is substantial. (Were it zero there would be no shadowing.) There are two basic ways in which one can estimate the size of this cross section. In the 3 quark model of a nucleon (2 quarks to a pion), if $\sigma(\pi - N) \sim 26$ mb then $\sigma(\text{parton} - N) \sim 13$ mb. Probably, however, there is a large number of constituent partons in each nucleon and they act coherently in nucleon-nucleon scattering. Nucleon-nucleon scattering can then be considered as the scattering of two disks of radius R for which $\sigma_T \sim 4R^2$. The parton-nucleon total cross section would then be 1/4 as large (the individual parton having a very small radius and the nucleonic partons still acting together coherently as a disk of radius R). This estimate gives $\sigma_T(\text{parton} - N) \sim 9$ mb. In either case the shadowing is negligible. Of course, if the partons of the single nucleon failed to act together coherently in parton-nucleon scattering the cross section would be extremely small. We can state these same considerations another way. The pointlike single step diagram will be shadowed only to the extent that non-interacting parton pairs propagate between the nucleons and contribute to the nuclear binding. (Interacting partons in the form of rho's etc. are of course important in the nuclear binding and these shadow the six point single step process.) Thus the amount of shadowing is correlated with the ability of a parton to escape from a nucleon. On the other hand, should a bound state

model be found in which the partons are unable to escape from the nucleon there would be no shadowing of the pointlike piece under consideration.

Secondly there is an important effect which arises from the interplay between the nuclear and parton physics. The nuclear physics is such that the nucleons can never be far off shell. This is a direct result of the small binding energy of the nucleus. (If a nucleon is forced too far off shell the nucleus breaks apart.) We shall see that this forces the partons in the two step process to be far off shell; this in turn causes the parton-proton scattering amplitude to vanish. (This vanishing is the basic assumption of parton models with exact scaling and is closely analogous to the nuclear physics requirement that the nucleons be nearly on shell.)

The most convenient way in which to keep covariant effects is, surprisingly, to perform the analysis in an infinite momentum frame using old fashioned perturbation theory. (See Fig. 7b for notation.) The degree to which the nucleons are off shell is measured by the energy denominators $E-E_1$ and $E-E_5$.

Referring to Fig. 7b we define our infinite momentum frame by (see Ref. 24) $P \rightarrow \infty$ with

$$q = \left(\frac{M\nu}{2P}, \vec{q}_1 - \frac{M\nu}{2P} \right), P_{\text{nucleus}} = \left(P + \frac{M_D^2}{2P}, \vec{0}, P \right)$$

$M = \text{nucleon mass}, \quad M_D = \text{deuteron mass}$

$$P_y = \left(yP + \frac{M^2 + p_1^2}{2yP}, \vec{p}_1, yP \right), P_{1-y} = \left((1-y)P + \frac{M^2 + p_1^2}{2(1-y)P}, -\vec{p}_1, (1-y)P \right)$$

$\text{and } y \rightarrow y' \quad p_1 \rightarrow p_1'$

$$P_{\delta x} = \left(\delta x P + \frac{\lambda^2 + k^2}{2\delta x P}, \vec{k}_1, \delta x P \right) \quad (\text{II. 1})$$

$\delta = y - y' \quad \lambda = \text{parton mass}$

One then obtains the following results: (the usual factor of $2P$ is understood here and below)

$$E - E_1 = M_D^2 - \frac{M^2 + p_1^2}{y(1-y)} = \frac{M^2(4y(1-y)-1)-p_1^2}{y(1-y)} + 2M\epsilon_B \quad (\text{II. 2})$$

$$E - E_5 = \frac{M^2(4y'(1-y')-1)-p_1'^2}{y'(1-y')} + 2M\epsilon_B$$

$\epsilon_B =$ binding energy

The requirement that these energy differences be small gives

$$y \approx \frac{1}{2} + 0(\epsilon_B/M) \quad p_1^2 \approx 0 + 0(\epsilon_B/M) \quad (\text{II. 3})$$

$$y' \approx \frac{1}{2} + 0(\epsilon_B/M) \quad p_1'^2 \approx 0 + 0(\epsilon_B/M)$$

We must also compute the energy differences $E_1 - E_2$ and $E_5 - E_4$ which measure the extent to which the partons are off shell as they emerge from the scattering.

$$E_1 - E_2 \approx \frac{-M^2\delta}{yy'} - \frac{\lambda^2 + k_1^2}{\delta x(1-x)} \quad (\text{using } p_1 \approx 0)$$

$$E_5 - E_4 \approx \frac{-M^2\delta}{(1-y')(1-y)} - \frac{\lambda^2 + k_1^2}{\delta x(1-x)} \quad \left(p_1' \approx 0 \right) \quad (\text{II. 4})$$

At this point one should notice:

(1) that since all intermediate particles must be forward moving in the infinite momentum frame, $\delta > 0$ is required,

(2) that this implies

$$E - E_1 < 0 \quad E - E_2 < 0 \quad E - E_4 < 0 \quad E - E_5 < 0, \text{ and} \quad (\text{II. 5})$$

(3) that we are working in the high energy approximation. That is, we have replaced the structured parton-proton scattering amplitudes by their approximate

net contribution at high energy which is presumably purely positive imaginary. (We shall verify shortly in II-10 that the appropriate energy is in fact large if ν is large.) In order for this two step process to shadow the one step process it must have an overall contribution of $-i$. Given the above approximation to the scattering amplitudes it is thus necessary that we be able to obtain a $+i$ from the only remaining energy denominator $E-E_3$. Since $E-E_1 \approx 0$,

$$E_1 - E_3 \approx -\frac{M^2 \delta}{yy'} + 2M\nu - \frac{\lambda^2 + (k_\perp + q_\perp)^2}{\delta x} - \frac{\lambda^2 + k_\perp^2}{\delta(1-x)} \quad (\text{II. 6})$$

For convenience we write this in terms of the two-parton invariant mass in this intermediate state, \mathcal{M} :

$$\mathcal{M}^2 + Q^2 = \frac{\lambda^2 + (q_\perp + k_\perp)^2}{x} + \frac{\lambda^2 + k_\perp^2}{(1-x)} \quad (\text{II. 7})$$

$$Q^2 = q_\perp^2 = -q^2 .$$

Then

$$E_1 - E_3 \approx -\frac{M^2 \delta}{yy'} + 2M\nu - \frac{(\mathcal{M}^2 + Q^2)}{\delta} \quad (\text{II. 8})$$

This quantity must be positive if any shadowing is to take place, i. e., if we are to be able to pick up an imaginary contribution from this energy denominator.

Thus,

$$\delta \geq \frac{(\mathcal{M}^2 + Q^2)}{2M\nu} \quad (\text{large } \nu \text{ solution}) . \quad (\text{II. 9})$$

Since we already know that δ wants to be as small as possible, the equality must in fact hold. Note that this implies

$$s_{\text{parton-proton}} \sim (y - \delta x) \left(\frac{M^2}{y} - \frac{\lambda^2 + k_\perp^2}{\delta x} \right) \approx -\frac{1}{2} \frac{\lambda^2 + k_\perp^2}{x} \frac{2M\nu}{(\mathcal{M}^2 + Q^2)} \quad (\text{II. 10})$$

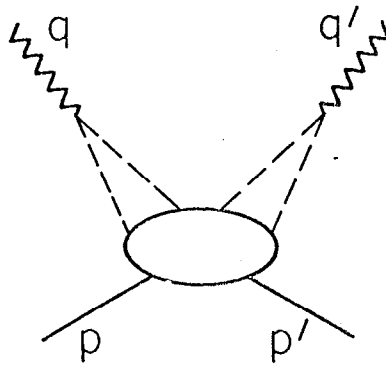
The nuclear physics alone will cause the process to vanish if ν is not large as δ cannot be small. If ν is large then δ can be small but then

$$E_5 - E_4 \approx E_1 - E_2 \approx -2M\nu \left[\frac{\lambda^2 + k_1^2}{x(1-x)(M^2 + Q^2)} \right] \quad (\text{II. 11})$$

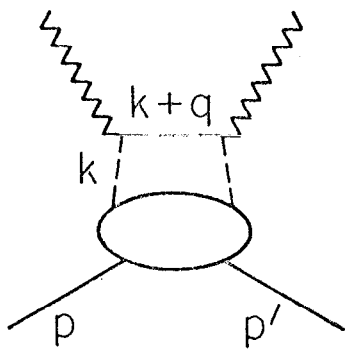
i. e. , the partons have been forced to go far off shell in this case. This causes the parton-proton amplitudes to vanish and again shadowing cannot occur.

There will of course be small corrections to the above discussion due to the real contributions to the coherent parton-proton scattering amplitudes from $f-A_2$ trajectories. They are however too small to have a measurable effect upon the above considerations.

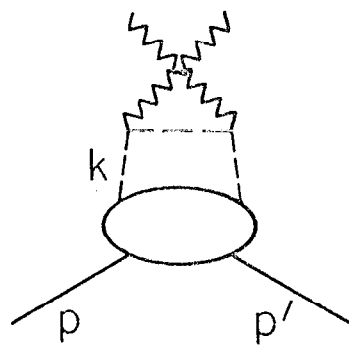
Thus in this appendix we have given two separate reasons as to why the parton pointlike contributions to the one step process should not be shadowed by the corresponding two step process.



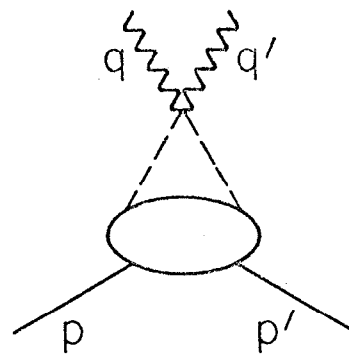
(a)



(b)



(c)



(d)

2015A1

Fig. 1

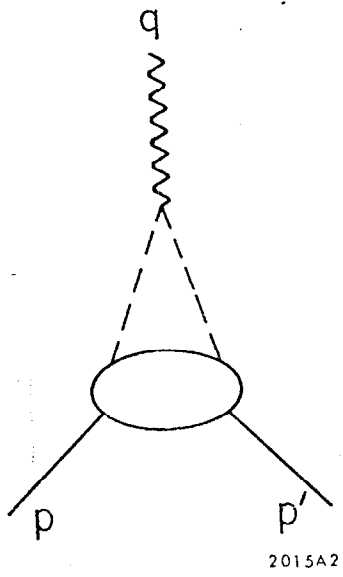
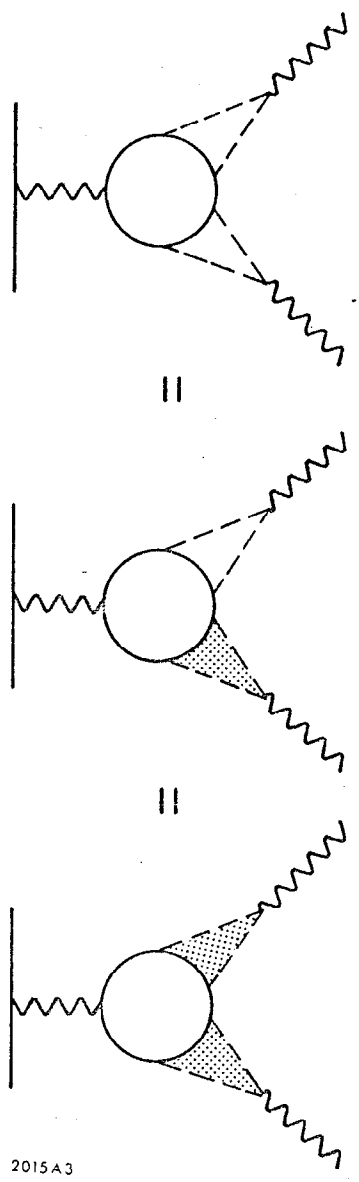


Fig. 2



2015A3

Fig. 3

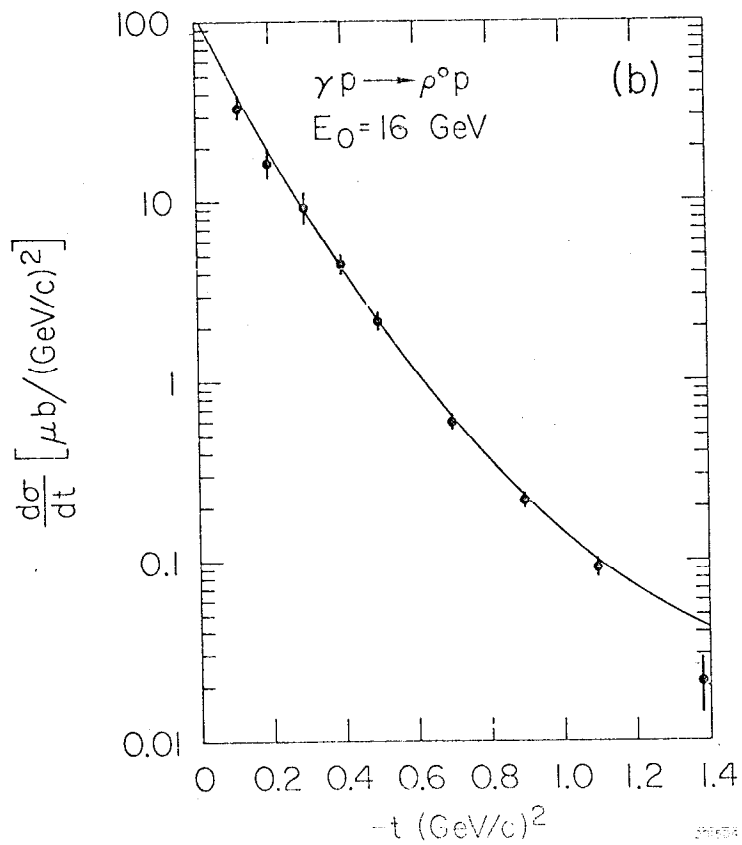
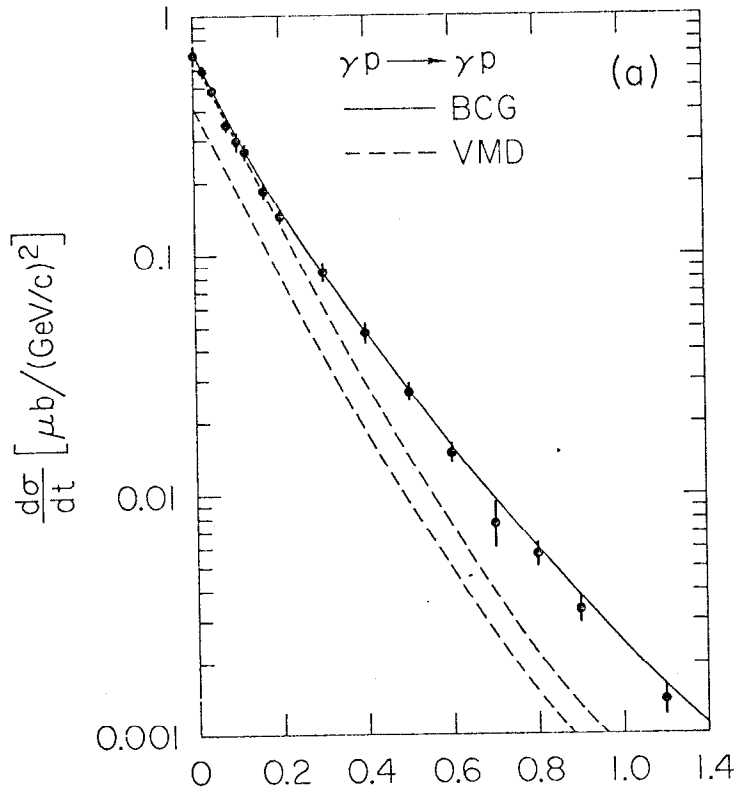
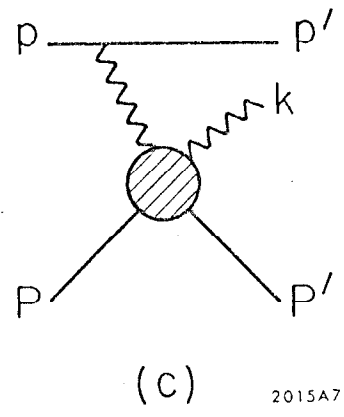
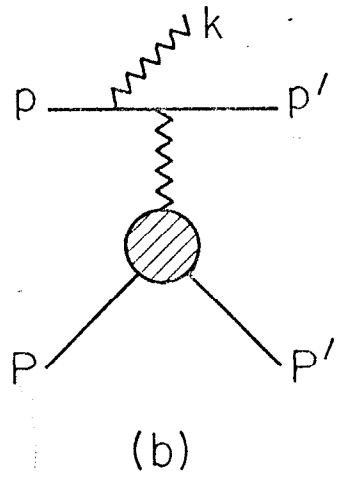
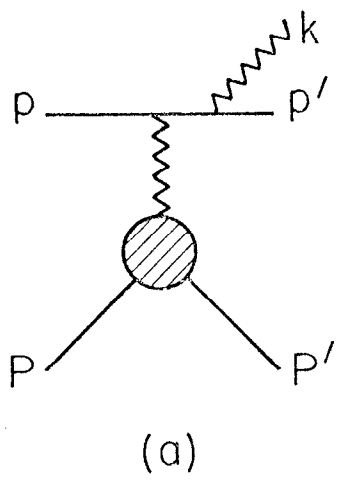


Fig. 4



2015A7

Fig. 5

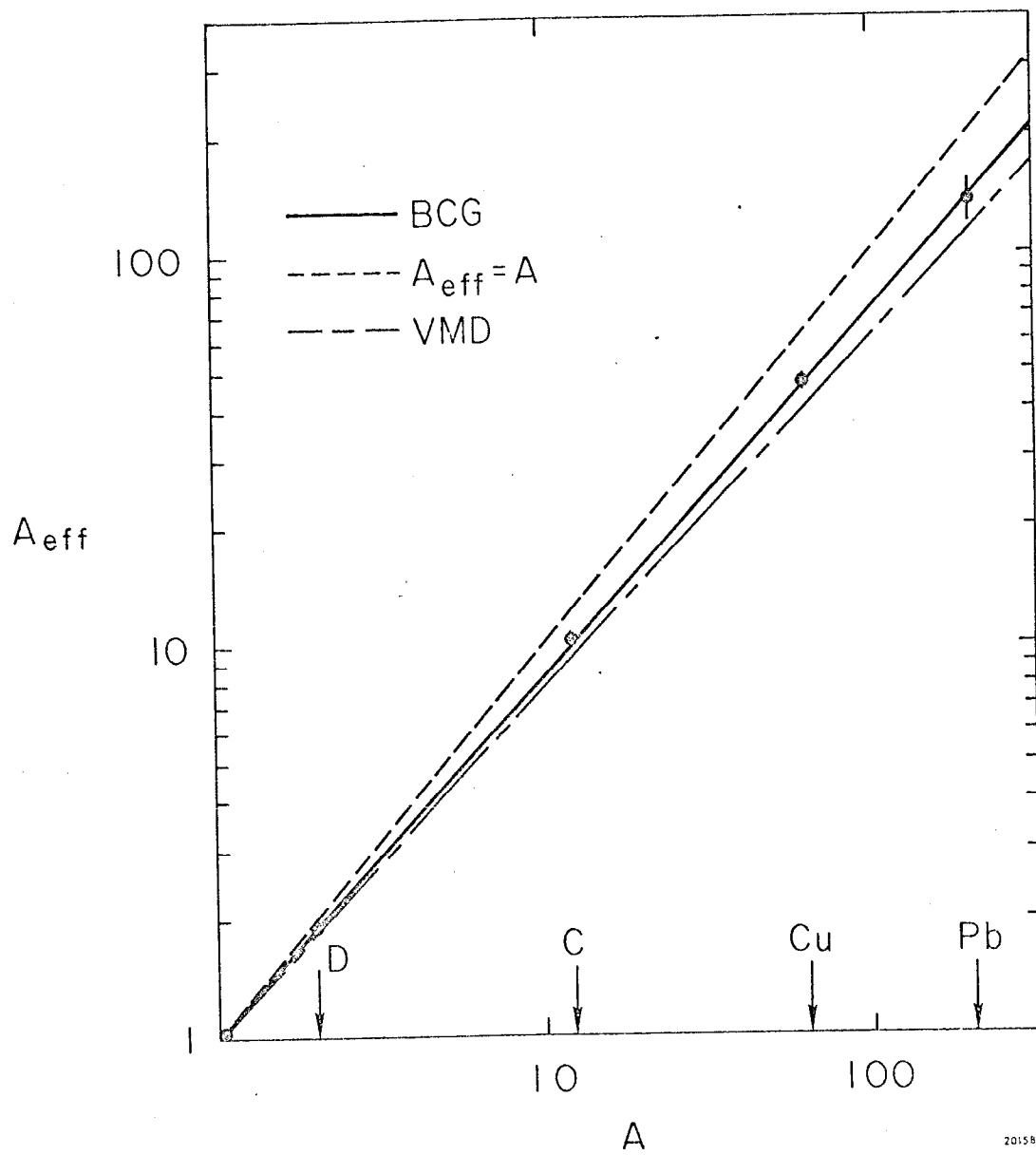
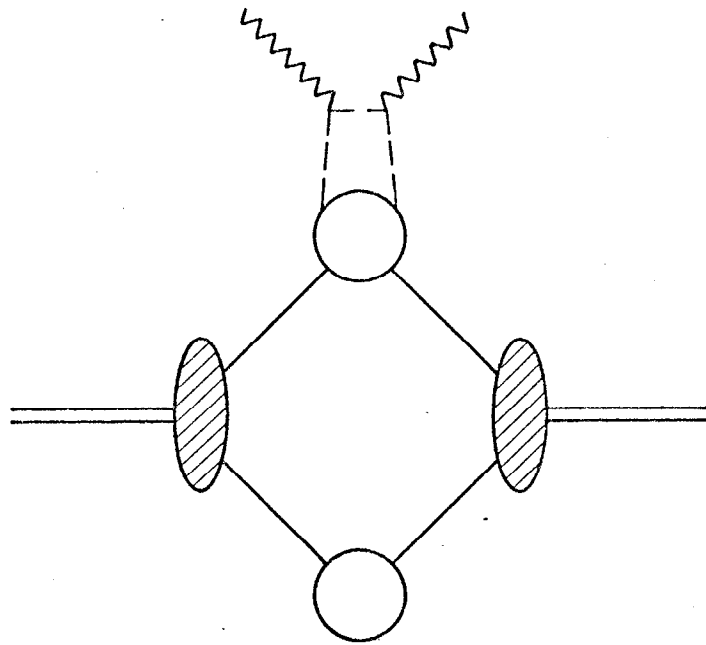
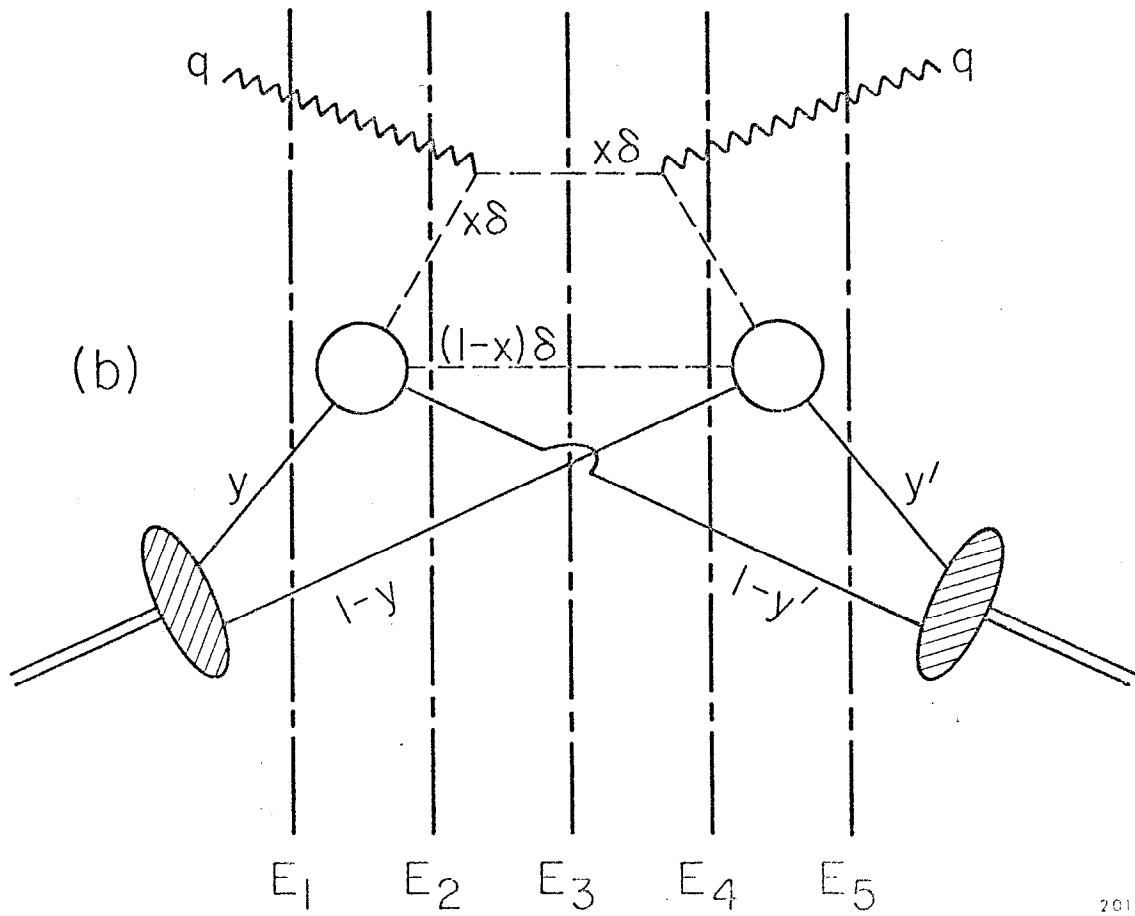


Fig. 6

(a)



(b)



2015A5

Fig. 7